

# Cooperativity in Two-State Protein Folding Kinetics

Thomas R. Weikl<sup>1,2,\*</sup>, Matteo Palassini<sup>1,†</sup>, and Ken A. Dill<sup>1,‡</sup>

<sup>1</sup>*Department of Pharmaceutical Chemistry, University of California, San Francisco, California 94143-2240, USA*

<sup>2</sup>*Max-Planck-Institut für Kolloid- und Grenzflächenforschung, 14424 Potsdam, Germany*

We present a solvable model that predicts the folding kinetics of two-state proteins from their native structures. The model is based on conditional chain entropies. It assumes that folding processes are dominated by small-loop closure events that can be inferred from native structures. For CI2, the src SH3 domain, TNfn3, and protein L, the model reproduces two-state kinetics, and it predicts well the average  $\Phi$ -values for secondary structures. The barrier to folding is the formation of predominantly local structures such as helices and hairpins, which are needed to bring nonlocal pairs of amino acids into contact.

## Keywords

Protein folding kinetics; two-state folding; folding cooperativity;  $\Phi$ -value analysis; effective contact order; loop-closure entropy; master equation

## I. INTRODUCTION

Protein folding kinetics is usually modeled in either of three ways. First, there are mass-action models that capture the amplitudes and decay rates of the exponentials in the folding or unfolding relaxation process [Ikai and Tanford 1971, Tsong et al. 1971, Dill and Chan 1997, Englander 2000]. Mass-action models are useful for cataloging the different types of kinetic behavior, but give no insight into molecular structures or mechanisms. Such models do not predict other experimental properties, such as  $\Phi$ -values. Second, there are all-atom or lattice model simulations that can explore sequence-structure relationships (see, e.g., [Duan and Kollman 1998, Shea and Brooks 2001, Daggett 2002]). They are usually limited by computational power to short time scales and to studying restricted conformational ensembles. Third, between these macroscopic and microscopic extremes, another type of model has recently emerged. This class of models uses knowledge of the native structure to infer the sequences of folding events [Munoz and Eaton 1999, Alm and Baker 1999, Galzitskaya and Finkelstein 1999, Debe and Goddard 1999, Shoemaker et al. 1999, Clementi et al. 2000, Hoang and Cieplak 2000, Li and Shakhnovich 2001, Portman et al. 2001, Ivankov and Finkelstein 2001, Alm et al. 2002, Klimov and Thirumalai 2002, Flammini et al. 2002, Bruscolini and Pelizzola 2002, Bruscolini and Cecconi 2002, Micheelsen et al. 2003].

Some of these models define partially folded states with one or two contiguous sequences of native-like ordered residues [Munoz and Eaton 1999, Alm and Baker 1999, Alm et al. 2002, Galzitskaya and Finkelstein 1999]. Others are based on a Go-model energy function that enforces the global stability of the native state [Clementi et al. 2000, Hoang and Cieplak 2000, Li and Shakhnovich 2001].

We describe here a folding model of the third type. Our model uses knowledge of the native structure to predict the kinetics. However, it differs from previous models in several respects. First, our model focuses on chain entropies and estimates loop lengths from the graph-theoretical concept of effective contact order ECO (see below). We follow time sequences of loop-closure events because we expect that these events reveal how the kinetics is encoded in the native structure. We assume that folding proceeds mostly through closures of small loops, and that large-loop closures are much slower and less important processes. Second, our model focuses on *contacts* within the chain, not on whether *residues* are native-like or not [Munoz and Eaton 1999, Alm and Baker 1999, Galzitskaya and Finkelstein 1999], because we think the formation of contacts is a more physical description of the folding process. Therefore, in our model partially folded states are characterized by formed contacts, not by contiguous stretches of native-like ordered residues as in other simple models. Third, the folding kinetics is described by a master equation that can be solved directly for the macrostates considered here, without stochastic simulations such as molecular dynamics or Monte Carlo. Hence the present treatment can handle the full spectrum of temporal events.

The present work is related to a recent model of protein zipping [Weikl et al. 2003a, Weikl et al. 2003b]. Our fundamental units of protein structure are *contact clusters*. A contact cluster is a collection of contacts that is localized on a contact map, corresponding roughly

\*email: Thomas.Weikl@mpikg-golm.mpg.de

†Present address: Laboratoire de Physique Théorique et Modèles Statistiques, Bât 100, Université Paris-Sud, 91405 Orsay - France; email: matteo@ipno.in2p3.fr

‡email: dill@maxwell.compbio.ucsf.edu

to the main structural elements of the native structure. Examples of contact clusters are turns,  $\alpha$ -helices,  $\beta$ -strand pairings, and tertiary pairings of helices. A central quantity in our models is the effective contact order (ECO) [Fiebig and Dill 1993, Dill et al. 1993]. The ECO is the length of the loop that has to be closed in order to form a contact, given a set of previously formed contacts or contact clusters. The premise is that the formation of the *nonlocal* contact clusters requires the prior formation of other, more *local*, clusters.

Our model predicts average  $\Phi$ -values for secondary structural elements that are in good agreement with the experimentally observed values for several two-state proteins. It shows that  $\Phi$ -value distributions can be understood from loop-closure events that are defined by the native topology of a protein. The importance of topology for routes and  $\Phi$ -values has also been previously noted by other groups [Munoz and Eaton 1999, Alm and Baker 1999, Alm et al. 2002, Clementi et al. 2000, Vendruscolo et al. 2001].

To compute the dynamics, we use a master equation. Several previous studies of the folding kinetics of lattice heteropolymer models have also been based on master equation methods [Leopold et al. 1992, Chan and Dill 1993, Cieplak et al. 1998, Ozkan et al. 2001, Ozkan et al. 2002, Ozkan et al. 2003, Schonbrun and Dill]. These methods have the advantage that they require no *ad hoc* assumptions about what the transition state is. The transition state emerges in a direct physical way from the solution to the master equation. However, the lattice models are too simplified to treat specific amino acid sequences or specific protein structures. Lattice models focus on transitions between *microstates*, the individual chain conformations, since these are the fundamental units of structure in such models. Our present master equation describes transitions between *macrostates*, defined by the contact clusters of a given protein structure. In this way, the present model aims to make closer contact with experiments.

## II. THE MODEL

### Contact clusters

To compute the folding kinetics, we start with the native contact map, the matrix in which element  $(i, j)$  equals 1 if the residues  $i$  and  $j$  are in contact, and equals 0 otherwise. Two residues are defined as being in contact if the distance between their  $C_\alpha$  or  $C_\beta$  atoms is less than 6 Angstroms.

Next, we divide the native contact map into contact clusters. Each contact cluster corresponds to a structural element of the protein. Two contacts  $(i, j)$  and  $(k, l)$  are defined as being in the same cluster if they are close together on the contact map, according to the distance criterion that  $|i - k| + |j - l| \leq 4$ . We define two types

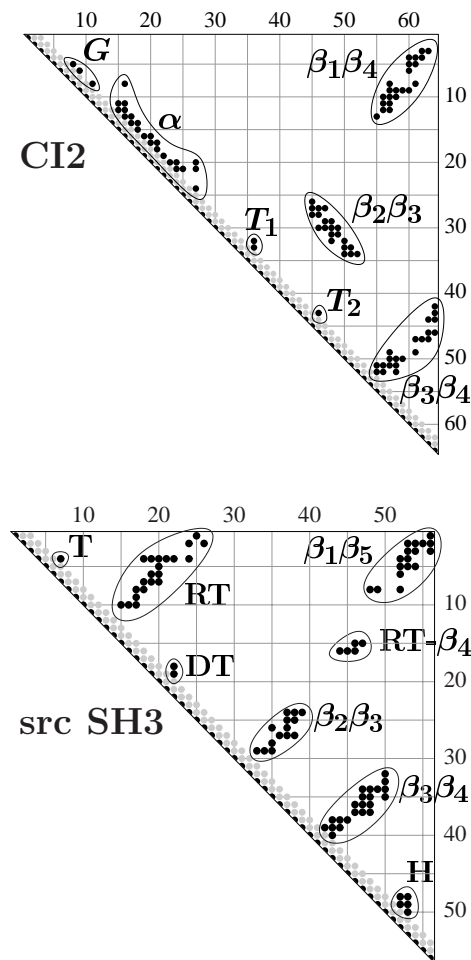


FIG. 1: Native contact maps and contact clusters for CI2 and the src SH3 domain.

of clusters: local and nonlocal. Clusters are *local* if they contain at least one local contact  $(i, j)$  having contact order  $CO = |i - j| \leq 6$ . Local clusters include helices, turns, or  $\beta$ -hairpins, for example. A cluster is *nonlocal* if it has no local contacts; examples include  $\beta$ -strand pairings other than hairpins, and the tertiary interactions of helices. To qualify as nonlocal, a cluster must also have more than two contacts; isolated nonlocal contacts are not considered to be clusters. Similarly, we do not consider as contributing to clusters any ‘peripheral’ contacts  $(i, j)$  with a minimum distance  $|i - k| + |j - l| = 4$  to the other contacts in the cluster. In general, typical contact maps have only a few isolated nonlocal or peripheral contacts. Fig. 1 shows examples of clusters, specifically for chymotrypsin inhibitor 2 (CI2) and the src SH3 domain. By our criteria, CI2 has 5 local clusters and 2 nonlocal clusters ( $\beta_2\beta_3$  and  $\beta_1\beta_4$ ), and the src SH3 domain has 6 local clusters and 2 nonlocal clusters ( $RT-\beta_4$  and  $\beta_1\beta_5$ ).

## States and free energies

We assume that each cluster is either formed or not; we neglect partial degrees of formation. Thus, for a protein with  $M$  clusters, there are  $2^M$  possible states that describe the progression to the native state. Each of these macrostates is characterized by a vector  $n = \{n_1, n_2, \dots, n_M\}$ , where  $n_i = 1$  indicates that cluster  $i$  is formed and  $n_i = 0$  indicates that cluster  $i$  is not formed.

In our model, the free energy of the protein as a function of the state  $n$  of cluster formation is given by:

$$F_n = \sum_{i=1}^M n_i [c \cdot \ell_i(n) + f_i] \quad (1)$$

Each cluster  $i$  that is formed ( $n_i = 1$ ) contributes to the free energy  $F_n$  of the state  $n$  with two terms: A state-dependent free energy of loop closure  $c \cdot \ell_i(n)$  ('initiation' free energy), and a free energy  $f_i$  for forming the cluster contacts ('propagation' free energy). Here,  $c$  is a loop-closure parameter. The quantity  $\ell_i = \ell_i(n)$  is the *initiation ECO* [Weikl et al. 2003a] for cluster  $i$ . The initiation ECO of a cluster is the length of the smallest loop that must be closed in order to form that cluster from the other existing clusters. For a local cluster, the initiation ECO is the smallest CO among the contacts. For a non-local cluster, the initiation ECO depends on the presence of other clusters in the state  $n$ .

In general, the initiation ECO also depends on the sequence through which those clusters are formed. However, in order to apply the master equation formalism, we need a free energy and thus we require a definition of initiation ECO that is only a function of state. For this purpose, we use the following scheme. If only one nonlocal cluster is formed in a certain state, the initiation ECO of that cluster is the smallest ECO among the cluster contacts, given all the local clusters formed in that state. If multiple nonlocal clusters are present in a state, we consider all the possible sequences along which these clusters can form, and determine the one having the smallest sum of ECOs. For instance, for a state with two nonlocal clusters  $C_i$  and  $C_j$ , there are two sequences: (1)  $C_i \rightarrow C_j$ , and (2)  $C_j \rightarrow C_i$ . The minimum ECOs for the clusters are determined sequentially:  $\ell_i^{(1)}$  and  $\ell_j^{(1)}$  along sequence (1), and  $\ell_i^{(2)}$  and  $\ell_j^{(2)}$  along sequence (2). If  $\ell_i^{(1)} + \ell_j^{(1)}$  is smaller than  $\ell_i^{(2)} + \ell_j^{(2)}$ , the initiation ECOs  $\ell_i$  and  $\ell_j$  of the clusters  $i$  and  $j$  in the given state are taken to be  $\ell_i^{(1)}$  and  $\ell_j^{(1)}$ . The initiation ECOs  $\ell_i$  and  $\ell_j$  are an estimate for the smallest loop lengths required to form the two clusters in the state.

In eq. (1), the free energy cost of the loops is estimated by a simple linear approximation in the loop length. This is not unreasonable since the range of relevant ECOs only spans roughly one order of magnitude, from about  $\ell \simeq 3$  to  $\ell \simeq 30$  or 40. In general, determining the free energy of a chain molecule with multiple constraints or contacts is a complicated and unsolved problem. For

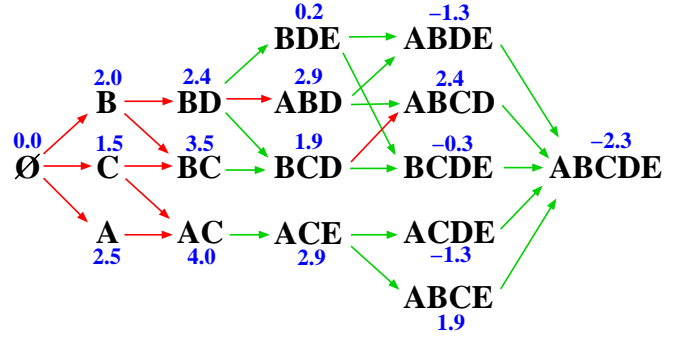


FIG. 2: Energy landscape for the src SH3 domain as a function of the 5 major clusters (A) RT, (B)  $\beta_2\beta_3$ , (C)  $\beta_3\beta_4$ , (D) RT- $\beta_4$ , and (E)  $\beta_1\beta_5$ . Here, BD, for example, means that only clusters B and D are formed. The free energies given by eq. (1) are shown in blue (the units are  $k_B T$ ). Red arrows indicate uphill steps in folding direction, green arrows downhill steps. For clarity, states with free energies larger than 4  $k_B T$  are neglected.

the simpler problem of hairpin-like loop closures, several estimates have been given in the literature (see, e.g., [Chan and Dill 1990, Galzitskaya and Finkelstein 1999, Ivankov and Finkelstein 2001]).

In principle, this model could treat the detailed energetics of each folding route, if each of the  $M$  clusters were characterized by its own free energy  $f_i$ . But here we consider a simpler version of the model. We assume that there are only two parameters for the free energy of formation:  $f_i = f_l$  for propagating any local cluster, and  $f_i = f_{nl}$  for propagating any nonlocal cluster. To obtain two-state folding and agreement with experimental  $\Phi$ -values, we find that  $f_l$  must be nonnegative and  $f_{nl}$  must be negative. This is consistent with the experimental observation that local structures, such as helices or  $\beta$ -hairpins, are generally unstable in isolation. Similar in spirit, the diffusion-collision model of Karplus and Weaver assumes that microdomains, e.g. helices, are individually unstable [Karplus and Weaver 1976, Karplus and Weaver 1994]. Thus, the rate-limiting barrier to folding in our model turns out to be the formation of mostly local structures needed to reduce the ECOs of nonlocal clusters. The driving force for overcoming this barrier is the favorable free energy  $f_{nl}$  of assembling the nonlocal clusters.

The predicted free energy landscape of the src SH3 domain is shown in Fig. 2, using the parameters  $f_l = 0$  and  $c = 0.5 k_B T$ , where  $k_B T$  is Boltzmann's constant  $\times$  temperature. The value of  $f_{nl}$  is chosen so that the equilibrium probability that the two nonlocal clusters RT- $\beta_4$  and  $\beta_1\beta_5$  are both folded ('native state') is 0.9, which gives  $f_{nl} = -6.6 k_B T$  for src SH3. With these parameter settings, we obtain a good agreement with average experimental  $\Phi$ -values for the src SH3 domain and other two-state folders (see below). For clarity, we show in the figure only a reduced set of states based on the 5 major clusters RT,  $\beta_2\beta_3$ ,  $\beta_3\beta_4$ , RT- $\beta_4$ , and  $\beta_1\beta_5$ . The three

small clusters T, DT, and H have negligible effects on the folding kinetics and on the  $\Phi$ -values. Only states differing by the formation of a single cluster are kinetically connected. The uphill steps in this model either are steps in which a local cluster is formed, or steps involving high ECOs. The downhill steps are steps in which a nonlocal cluster is formed with a low ECO, or steps in which a local cluster significantly reduces the ECOs of previously formed nonlocal clusters. The model predicts two main folding routes. Along the upper route (E)  $\beta_1\beta_5$  folds after (D) RT- $\beta_4$ ; along the lower route, they form in the opposite order. Along these routes, the barriers (highest free energies states) are the states in which two clusters are formed: BD and BC for the upper route, and AC for the lower route.

### Master equation

In this section, we describe the folding dynamics. We use the master equation,

$$\frac{dP_n(t)}{dt} = \sum_{m \neq n} [w_{nm}P_m(t) - w_{mn}P_n(t)], \quad (2)$$

which gives the time evolution of the probability  $P_n(t)$  that the protein is in state  $n$  at time  $t$ . Here,  $w_{nm}$  is the transition rate from state  $m$  to  $n$ . The master equation can be written in matrix form

$$\frac{d\mathbf{P}(t)}{dt} = -\mathbf{W}\mathbf{P}(t) \quad (3)$$

where  $\mathbf{P}(t)$  is the vector with elements  $P_n(t)$ , and the matrix elements of  $\mathbf{W}$  are given by

$$W_{nm} = -w_{nm} \quad \text{for } n \neq m; \quad W_{nn} = \sum_{m \neq n} w_{mn}. \quad (4)$$

The transition rates are given in terms of the free energies by

$$w_{nm} = \frac{\delta_{|n-m|,1}}{t_o} \left[ 1 + \exp\left(\frac{F_n - F_m}{k_B T}\right) \right]^{-1} \quad (5)$$

where  $t_o$  is a reference time scale. The only transitions that are assigned to have nonzero rates  $w_{nm}$  are those incremental steps that change the state  $n$  by a single cluster unit. This is enforced by the term  $\delta_{|n-m|,1}$  in eq. (5) where the Kronecker  $\delta_{i,j}$  is one for  $i = j$  and zero otherwise. The condition  $|n - m| = 1$  is only satisfied by pairs of states  $n = \{n_1, \dots, n_M\}$  and  $m = \{m_1, \dots, m_M\}$  with  $n_k \neq m_k$  for a single cluster  $k$ , and with  $n_k = m_k$  for all other clusters. The transition rates (5) satisfy detailed balance,  $w_{nm}P_m^e = w_{mn}P_n^e$  where  $P_n^e \sim \exp[-F_n/(k_B T)]$  is the equilibrium weight for the state  $n$ . We have chosen here the ‘Glauber dynamics’ with  $w_{nm} \sim (1 + \exp[(F_n - F_m)/(k_B T)])^{-1}$ . Another standard choice satisfying detailed balance is the

Metropolis dynamics, which should lead to equivalent results.

The detailed balance property of the transition rates implies that the eigenvalues of the matrix  $\mathbf{W}$  are real. One of the eigenvalues is zero, corresponding to the equilibrium distribution, while all other eigenvalues are positive [van Kampen 1992]. The solution to the master equation is given by

$$\mathbf{P}(t) = \sum_{\lambda} c_{\lambda} \mathbf{Y}_{\lambda} \exp[-\lambda t] \quad (6)$$

where  $\mathbf{Y}_{\lambda}$  is the eigenvector corresponding to the eigenvalue  $\lambda$ , and the coefficients  $c_{\lambda}$  are determined by the initial condition  $\mathbf{P}(t = 0)$ . For  $t \rightarrow \infty$ , the probability distribution  $\mathbf{P}(t)$  tends towards the equilibrium distribution  $\mathbf{P}^e \sim \mathbf{Y}_0$  where  $\mathbf{Y}_0$  is the eigenvector with eigenvalue  $\lambda = 0$ .

Solving the master equation gives a set of  $2^M$  eigenvalues, each with its associated eigenvector. Each eigenvalue represents a relaxation rate. As initial conditions at  $t = 0$ , we start from the state in which no clusters are formed. This corresponds to folding from high temperatures or high denaturant concentrations.

## III. RESULTS

### The cooperativity in two-state kinetics

The signature of two-state kinetics is the existence of one slow relaxation process (described by a single exponential), separated in time from  $2^M - 1$  fast relaxations (a ‘burst’ phase). Fig. 3 shows the eigenvalue spectra for CI2 and the src SH3 domain, based on using the parameters  $c = 0.5 k_B T$ , local cluster free energy  $f_l = 0$ , and a nonlocal cluster free energy chosen so that the equilibrium ‘native’ population with all nonlocal clusters formed has probability 0.9. The latter condition leads to  $f_{nl} = -7.9 k_B T$  for CI2, and  $f_{nl} = -6.6 k_B T$  for src SH3. Fig. 4 shows the predicted folding dynamics for the src SH3 domain.

The spectra in Fig. 3 show that for these proteins, the eigenvalues do indeed separate into a slow single-exponential step and a burst phase, consistent with the experimental observation of two-state behavior. The slowest relaxation rate  $\lambda_1$  is about one order of magnitude smaller than the other nonzero eigenvalues (see Fig. 3). At times  $t \gtrsim 1/\lambda_1$ , the probability distribution (6) is well approximated by  $\mathbf{P}(t) \simeq c_0 \mathbf{Y}_0 + c_1 \mathbf{Y}_1 \exp[-\lambda_1 t]$  where  $\mathbf{Y}_0$  is the eigenvector with eigenvalue 0, which characterizes the equilibrium state, and  $\mathbf{Y}_1$  is the eigenvector with eigenvalue  $\lambda_1$ .

The typical time evolution of the folding process predicted by the model is as follows. We have two time scales,  $t \simeq t_o$  and  $t_F \simeq 1/\lambda_1$ . Time  $t_o$  is a characteristic of the burst phase in the model and  $t_F$  is the single-exponential folding time. At the earliest times,  $t < t_o$ ,

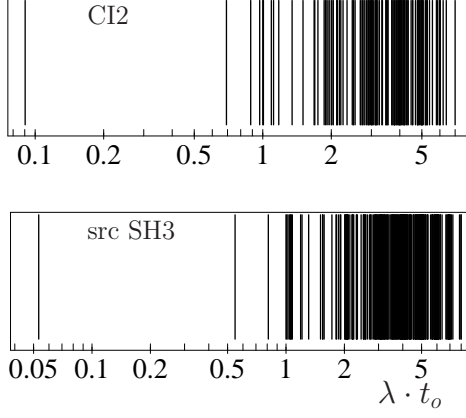


FIG. 3: Eigenvalue spectra for CI2 and the src SH3 domain in units of  $1/t_o$  where  $t_o$  is the reference time scale for the transition rates (5).

single local clusters start to form: examples are the clusters A, B, and C of the src SH3 domain, see Fig. 2. As shown in Fig. 4, on this time scale, each cluster is only weakly populated, with a probability less than 10%. Any structures having larger-scale organization – cluster pairs, triplets, etc. – have negligible populations. At intermediate times,  $t_F \gtrsim t \gtrsim t_o$ , there is a crossover from the burst phase to the single-exponential folding process. During these intermediate times, cluster pairs (AC, BC, BD) begin to form. Fig. 2 shows that these pairwise clusters are the barrier events, i.e., they represent the conformational states of maximum free energy obtained during folding. Finally, on the longest time scale,  $t \simeq t_F$ , the pairwise and triplet clusters reach sufficiently high populations to assemble into multi-cluster complexes, proceeding downhill in free energy to the native structure.

What is the basis for the cooperativity of folding in our model, i.e. for the separation of time scales? First, the formation of local structures in our model reduces the loop-closure entropies for the formation of the nonlocal structures. Second, only the nonlocal structures have favorable propagation free energies  $f_i = f_{nl} < 0$ . Hence, the formation of the nonlocal structures stabilizes the overall fold, and thus also the local structures. The barrier arises from the positive free energies in eq. (1) due to the formation of local structures and loops (see Fig. 2). Interestingly, if we set the free energies for local structure formation to be negative by several  $k_B T$ , we obtain fast multi-exponential downhill folding, without a barrier. Based on experiments and theory, such downhill folding has been recently postulated for the protein BBL [Garcia-Mira et al. 2002].

To understand the cooperative folding in the model, it is instructive to turn off the loop-closure term in eq. (1) by setting  $c = 0$ . Then all  $M$  clusters are independent of each other. In that case, there is no cooperativity. It can be shown that the matrix  $\mathbf{W}$  then has the eigen-

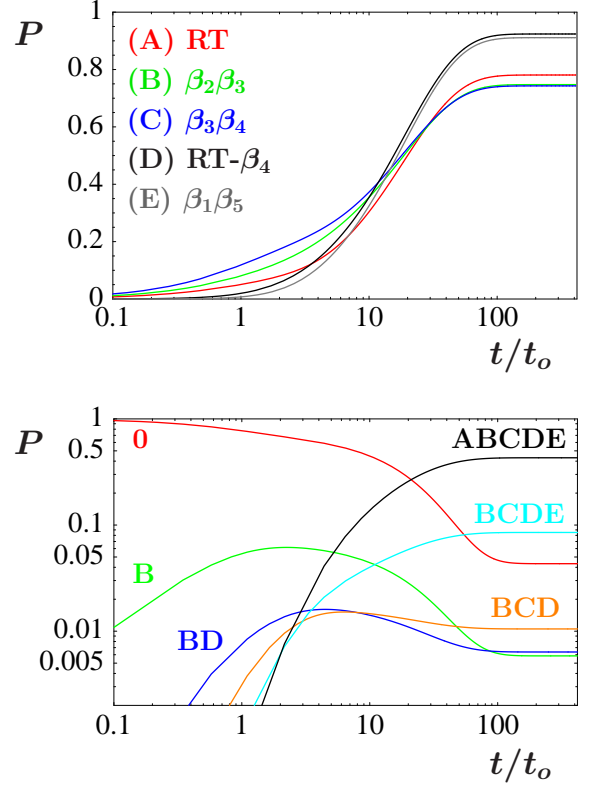


FIG. 4: (Top) Time evolution of the formation probability  $P$  for the major *clusters* of the src SH3 domain during folding (see Fig. 1). (Bottom) Time evolution of *state* probabilities for the exemplary path  $0 \rightarrow B \rightarrow BC \rightarrow BCD \rightarrow BCDE \rightarrow ABCDE$  of the src SH3 domain (see also Fig. 2). The initial state at time  $t = 0$  is the denatured state in which none of the clusters is formed.

values  $\lambda = j/t_o$  where  $j$  is an integer between 0 and  $M$ , the number of clusters. Each of these eigenvalues has a population that is given by the binomial coefficient  $j!/[j!(M-j)!]$ . This gives a broad non-two-state spectrum. Hence, the separation of time scales – and the two-state cooperativity – arise in this model from the coupling of the clusters via the loop-closure term in eq. (1).

To see the magnitude of the barrier, note that the folding rate  $\lambda_1$  is related to the height of the energy barrier on the folding landscape. For comparison, consider a mass-action model with three states  $D \leftrightarrow T \leftrightarrow N$  (denatured state, ‘transition’ state, native state) and transition rates as in eq. (5). The folding rate is given, to a very good approximation, by  $(1/2)t_o^{-1} \exp[-F_b^\ddagger/(k_B T)]$  for barrier energies  $F_b^\ddagger = F_T^\ddagger - F_D^\ddagger \gg k_B T$ . The factor of  $1/2$  comes from the fact that a molecule in state  $T$  can jump both to  $D$  and  $N$ , with almost equal probability, since both sides of high-barrier transition states are steep downhill. Now, for the energy landscape of the src SH3 domain shown in Fig. 2, the minimum barrier

Table 1: Maximum probability  $P_{max}$  and  $\mathbf{Y}_1$  elements for transient states of the src SH3 domain.

state	$P_{max}$	$\mathbf{Y}_1$ element
C	0.13	0.21
B	0.062	0.10
A	0.047	0.08
BD	0.016	0.019
BC	0.010	0.017
AC	0.007	0.011
BCD	0.015	0.010
ABD	0.004	0.003
ACE	0.004	0.001

has free energy  $2.4 k_B T$  for state BD. The corresponding barrier crossing rate of  $(1/2)t_o^{-1} \exp[-2.4]$  is in good agreement with the folding rate  $\lambda_1 \simeq 0.05/t_o$  (see Fig. 3).

Experiments have been interpreted either as indicating that burst phases involve structure formation or that burst phases are processes of non-structured polymer collapse, depending on the protein and the experimental method [Englander 2000, Callender et al. 1998, Gruebele et al. 1998, Eaton et al. 1998, Parker and Marqusee 2000, Ferguson and Fersht 2003]. In our model, the burst phase is a process of structure formation. Non-structured collapse is beyond the scope, or resolution, of our model, because the model has only a single fully unstructured state – the state in which none of the clusters is formed. The burst phase in our model captures fast preequilibration events within the denatured state in response to initiating the folding conditions at  $t = 0$ . In the model, this denatured state is an ensemble of macrostates on one side of the barrier in the energy landscape (see Fig. 2). It is reasonable to assume that such preequilibration events within the denatured state exist also for real proteins. However, whether these events can be detected as burst phases in experiments should depend on the initial conditions, experimental probes, etc.

During folding or unfolding, certain conformations will be populated transiently. If the populations of those conformations are always small, we call them ‘hidden intermediates’ [Ozkan et al. 2002]. The population of a hidden intermediate conformation rises to a maximum,  $P_{max}$ , then falls as the protein ultimately becomes fully folded. The term ‘hidden’ means that  $P_{max}$  is always small enough that it does not contribute an additional kinetic phase; i.e., the folding kinetics is two-state. Here, we consider two quantities. (1) We compute  $P_{max}$  for the transient states. For simplicity, we consider only the 5 major clusters  $RT$ ,  $\beta_2\beta_3$ ,  $\beta_3\beta_4$ ,  $RT\text{-}\beta_4$ , and  $\beta_1\beta_5$ . (2) We look at the elements of the eigenvector  $\mathbf{Y}_1$ , the eigenvector corresponding to the smallest eigenvalue  $\lambda_1$ . These elements show how the various conformations grow and decay with rate  $\lambda_1$  as folding proceeds. Table 1 shows

that the maximum population  $P_{max}$  correlates well with the elements of  $\mathbf{Y}_1$ . For a typical route of src SH3, Fig. 4 (bottom) illustrates the decay of the denatured state and hidden intermediates and the growth of the native state, all with rate  $\lambda_1$ .

#### Average $\Phi$ -values for secondary structural elements

The effects of a mutation on the folding kinetics are often explored through experimental measurements of a  $\Phi$ -value, which is defined as

$$\Phi = -\frac{k_B T \ln(k'_f/k_f)}{\Delta G' - \Delta G} \quad (7)$$

where  $k_f$  is the folding rate of the native protein and  $\Delta G$  is its stability, and  $k'_f$  and  $\Delta G'$  are the corresponding quantities for the mutant protein.

Since the minimal structural units in our model are clusters of contacts, we do not calculate  $\Phi$ -values for single-residue mutations. Rather, we consider whole helices and strands as units. To compare with experiments, we average the experimental  $\Phi$ -values over all the residues composing a given secondary structural element.

To calculate average  $\Phi$ -values for secondary structures, we consider ‘mutations’ that change the free energy  $f_i$  of a contact cluster according to

$$\Delta f_i(j) = x_{ji}\epsilon \quad (8)$$

where  $x_{ji}$  is the fraction of residues of the secondary structural element  $j$  that are involved in contacts of the cluster  $i$ , and  $\epsilon$  is a small energy. For example, if the secondary structural element  $j$  contains  $m_1$  residues, and  $m_2 \leq m_1$  of these residues appear in contacts of the cluster  $i$ , we have  $x_{ji} = m_2/m_1$ . Note that  $0 \leq x_{ji} \leq 1$ , where the value  $x_{ji} = 1$  is obtained if the whole secondary structural element  $j$  has contacts in cluster  $i$ . Thus the  $\Phi$ -value for the secondary structural element  $j$  is given by eq. (7) with

$$\ln(k'_f/k_f) = \ln(\lambda'_1/\lambda_1) \quad (9)$$

where  $\lambda'_1$  is the smallest nonzero eigenvalue of the mutant with cluster free energies  $f_i \rightarrow f_i + \Delta f_i(j)$ , and

$$\Delta G' - \Delta G = \sum_i \Delta f_i(j) \quad (10)$$

For  $\epsilon \ll k_B T$ , we find that the calculated  $\Phi$ -values are nearly independent of  $\epsilon$ . We choose here  $\epsilon = 0.01 k_B T$ .

Predicted  $\Phi$ -values are compared with experiments in Fig. 5. The theoretical  $\Phi$ -values were calculated with the same parameters for all four proteins (see figure caption). The predicted values agree well with the experimental values. This comparison indicates that the folding kinetics of these proteins is dominated by generic features of the fold topology, rather than by the specific energetic

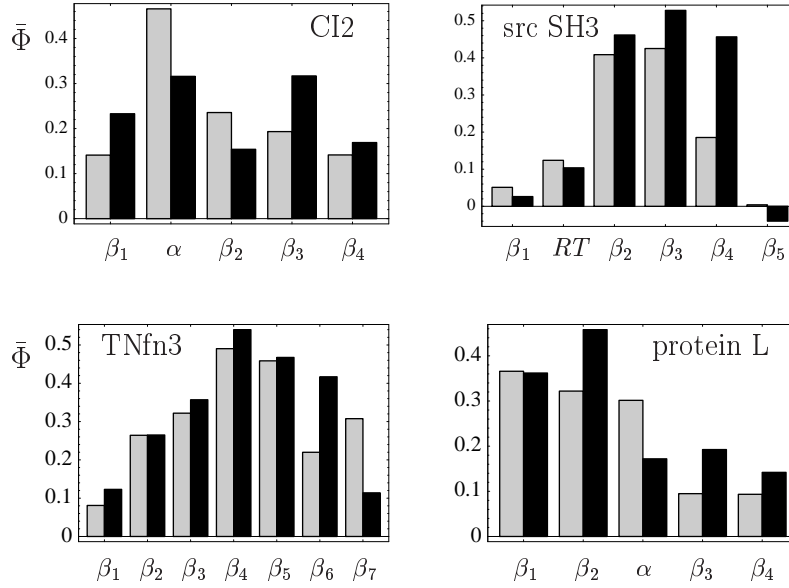


FIG. 5: Theoretical and average experimental  $\Phi$ -value distributions for the secondary structural elements of CI2, the src SH3 domain, TNfn3, and protein L. The parameter of the loop closure term is  $c = 0.5$ , and the free energy of the local clusters is  $f_l = 0$ . The free energy  $f_{nl}$  of the nonlocal clusters is chosen so that the probability that all nonlocal clusters are formed is 0.9 in equilibrium.

details – i.e., which residues form contacts, how much hydrogen bonds or hydrophobic interactions are worth, the details of sidechain packing, etc. In the case of protein G (see Fig. 6), the experimental  $\Phi$ -value distribution is largely reproduced by making the additional assumption that the  $\alpha$ -helix cluster has a free energy  $f_i = -2.0 k_B T$ , rather than the value  $f_i = 0 k_B T$  that we have otherwise used for local clusters (see Fig. 5). However, even without changing this parameter, the  $\Phi$ -value distribution reflects the features of the experimental distribution that the  $\Phi$ -values for the strands  $\beta_3$  and  $\beta_4$  are larger than those for  $\beta_1$  and  $\beta_2$ .

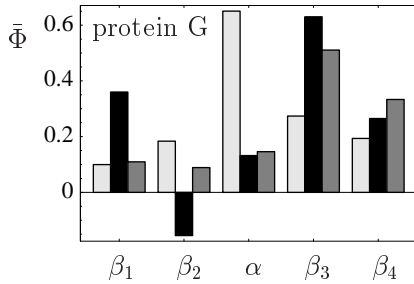


FIG. 6: Comparison of theoretical and experimental  $\Phi$ -value distributions. (Light grey): theoretical  $\Phi$ -values for the same parameters as in Fig. 5. (Black): average experimental  $\Phi$ -values. (Dark grey): theoretical  $\Phi$ -values when assuming that the free energy of the  $\alpha$ -helix cluster is  $f_i = -0.5 k_B T$ , deviating from the standard value  $f_l = 1.5 k_B T$  for the local clusters.

#### IV. CONCLUSIONS

We have developed a simple model of the folding kinetics of two-state proteins. The model aims to predict the folding rates of the fast and slow processes, the folding routes, and  $\Phi$ -values for a protein, if the native structure is given. The dominant folding routes are found to be those having small ECOs, i.e., steps that involve only small ‘loop closures’. The model parameters include:  $c$ , an intrinsic free energy for loop closure;  $f_l$ , the free energy for propagating contacts in local structures; and  $f_{nl}$ , the free energy for propagating nonlocal contacts. The model predicts that the barrier to two-state folding is the formation of local structural elements like helices and hairpins, and that the steps involving their assembly into larger and more native-like structure are downhill in free energy.

#### References

- Alm, E., and Baker, D. 1999. Prediction of protein- folding mechanisms from free-energy landscapes derived from native structures. *Proc. Natl. Acad. Sci. USA* **96**, 11305-11310.
- Alm, E., Morozov, A.V., Kortemme, T., and Baker, D. 2002. Simple physical models connect theory and experiment in protein folding kinetics. *J. Mol. Biol.* **322**, 463-476.
- Bruscolini, P., and Pelizzola, A. 2002. Exact solution of



- the Munoz-Eaton model for protein folding. *Phys. Rev. Lett.* **88**, 258101.
- Bruscolini, P., and Cecconi, F. 2003. Mean-field approach for a statistical mechanical model of proteins. *J. Chem. Phys.* **119**, 1248-1256.
- Callender, R.H., Dyer, R.B., Gilmanshin, R., and Woodruff, W.H. 1998. Fast events in protein folding: The time evolution of primary processes. *Annu. Rev. Phys. Chem.* **49**, 173-202.
- Chan, H.S., and Dill, K.A. 1990. The effects of internal constraints on the configurations of chain molecules. *J. Chem. Phys.* **92**, 3118-3135.
- Chan, H.S., and Dill, K.A. 1993. Energy landscapes and the collapse dynamics of homopolymers. *J. Chem. Phys.* **99**, 2116-2127.
- Cieplak, M., Henkel, M., Karbowski, J., and Banavar, J.R. 1998. Master equation approach to protein folding and kinetic traps. *Phys. Rev. Lett.* **80**, 3654-3657.
- Clementi, C., Nymeyer, H., and Onuchic, J.N. 2000. Topological and energetic factors: What determines the structural details of the transition state ensemble and "en-route" intermediates for protein folding? An investigation for small globular proteins. *J. Mol. Biol.* **298**, 937-953.
- Daggett, V. 2002. Molecular dynamics simulations of the protein unfolding/folding reaction. *Acc. Chem. Res.* **35**, 422-429.
- Debe, D.A., and Goddard, W.A. III. 1999. First principles prediction of protein folding rates. *J. Mol. Biol.* **294**, 619-625.
- Dill, K.A., Fiebig, K.M., and Chan, H.S. 1993. Cooperativity in protein-folding kinetics. *Proc. Natl. Acad. Sci. USA* **90**, 1942-1946.
- Dill, K.A., and Chan, H.S. 1997. From Levinthal to pathways to funnels. *Nat. Struct. Biol.* **4**, 10-19.
- Duan, Y., and Kollman, P.A. 1998. Pathways to a protein folding intermediate observed in a 1-microsecond simulation in aqueous solution. *Science* **282**, 740-744.
- Eaton, W.A., Munoz, V., Thompson, P.A., Henry, E.R., and Hofrichter, J. 1998. Kinetics and dynamics of loops,  $\alpha$ -helices,  $\beta$ -hairpins, and fast-folding proteins. *Acc. Chem. Res.* **31**, 741-753.
- Englander, S.W. 2000. Protein folding intermediates and pathways studied by hydrogen exchange. *Annu. Rev. Biophys. Biomol. Struct.* **29**, 213-238.
- Ferguson, N., and Fersht, A.R. 2003. Early events in protein folding. *Curr. Opin. Struct. Biol.* **13**, 75-81.
- Fiebig, K.M., and Dill, K.A. 1993. Protein core assembly processes. *J. Chem. Phys.* **98**, 3475-3487.
- Flammini A., Banavar, J.R., and Maritan, A. 2002. Energy landscape and native-state structure of proteins - A simplified model. *Europhysics Letters* **58**, 623-629.
- Galzitskaya, O.V., and Finkelstein, A.V. 1999. A theoretical search for folding/unfolding nuclei in three-dimensional protein structures. *Proc. Natl. Acad. Sci. USA* **96**, 11299-11304.
- Garcia-Mira, M.M., Sadqi, M., Fischer, N., Sanchez-Ruiz, J.M., and Munoz, V. 2002. Experimental identification of downhill protein folding. *Science* **298**, 2191-2195.
- Gruebele, M., Sabelko, J., Ballew, R., and Ervin, J. 1998. Laser temperature jump induced protein refolding. *Acc. Chem. Res.* **31**, 699-707.
- Hoang, T.X., and Cieplak, M. 2000. Sequencing of folding events in Go-type proteins. *J. Chem. Phys.* **113**, 8319-8328.
- Ikai, A., and Tanford, C. 1971. Kinetic evidence for incorrectly folded intermediate states in the refolding of denatured proteins. *Nature* **230**, 100-102.
- Ivankov, D.N., and Finkelstein, A.V. 2001. Theoretical study of a landscape of protein folding-unfolding pathways. Folding rates at midtransition. *Biochemistry* **40**, 9957-9961.
- Karplus, M., and Weaver, D.L. 1976. Protein-folding dynamics. *Nature* **260**: 404-406.
- Karplus, M., and Weaver, D.L. 1994. Protein-folding dynamics: The diffusion-collision model and experimental data. *Protein Science* **3**: 650-668.
- Klimov, D.K., and Thirumalai, D. 2002. Stiffness of the distal loop restricts the structural heterogeneity of the transition state ensemble in SH3 domains. *J. Mol. Biol.* **317**, 721-737.
- Leopold, P.E., Montal, M., and Onuchic, J.N. (1992). Protein folding funnels: A kinetic approach to the sequence-structure relationship. *Proc. Natl. Acad. Sci. USA* **89**, 8721-8725.
- Li, L., and Shakhnovich, E.I. 2001. Constructing, verifying, and dissecting the folding transition state of chymotrypsin inhibitor 2 with all-atom simulations. *Proc. Natl. Acad. Sci. USA* **98**, 13014-13018.
- Micheelsen, M.A., Rischel, C., Ferkinghoff-Borg, J., Guerois, R., and Serrano, L. 2003. Mean first-passage time analysis reveals rate-limiting steps, parallel pathways and dead ends in a simple model of protein folding. *Europhys. Lett.* **61**, 561-566.
- Muñoz, V., & Eaton, W.A. 1999. A simple model for calculating the kinetics of protein folding from three-dimensional structures. *Proc. Natl. Acad. Sci. USA* **96**, 11311-11316.



- Ozkan, S.B., Bahar, I., and Dill, K.A. 2001. Transition states and the meaning of  $\Phi$ -values in protein folding kinetics. *Nat. Struct. Biol.* **8**, 765-769.
- Ozkan, S.B., Dill, K.A., and Bahar, I. 2002. Fast-folding protein kinetics, hidden intermediates, and the sequential stabilization model. *Protein Sci.* **11**, 1958-1970.
- Ozkan, S.B., Dill, K.A., and Bahar, I. 2003. Computing the Transition State Populations in Simple Protein Models. *Biopolymers* **68**: 35-46.
- Parker, M.J., and Marqusee, S. 2000. A statistical appraisal of native state hydrogen exchange data: Evidence for a burst phase continuum? *J. Mol. Biol.* **300**, 1361-1375.
- Portman, J.J., Takada, S., and Wolynes, P.G. 2001. Microscopic theory of protein folding rates. I. Fine structure of the free energy profile and folding routes from a variational approach. *J. Chem. Phys.* **114**, 5069-5081.
- Schonbrun, J., and Dill, K.A. Why do proteins fold with single-exponential kinetics. Submitted
- Shea, J.-E., and Brooks III, C.L. 2001. From folding theories to folding proteins: A review and assessment of simulation studies of protein folding and unfolding. *Ann. Rev. Phys. Chem.* **52**, 499-535.
- Shoemaker, B.A., Wang, J., and Wolynes, P.G. 1999. Exploring structures in protein folding funnels with free energy functionals: The transition state ensemble. *J. Mol. Biol.* **287**, 675-694.
- Tsong, T.Y., Baldwin, R.L., and Elson, E.L. 1971. The sequential unfolding of ribonuclease A: Detection of a fast initial phase in the kinetics of unfolding. *Proc. Natl. Acad. Sci. USA* **68**, 2712-2715.
- van Kampen, N.G. 1992. *Stochastic processes in physics and chemistry*, (Elsevier, Amsterdam)
- Vendruscolo, M., Paci, E., Dobson, C.M., and Karplus, M. 2001. *Nature (London)* **409**, 641-645.
- Weikl, T.R., and Dill, K.A. 2003. Folding rates and low-entropy-loss routes of 2-state proteins. *J. Mol. Biol.* **329**, 585-598.
- Weikl, T.R., and Dill, K.A. 2003. Folding kinetics 2-state proteins: Effect of circularization, permutation, and crosslinks. *J. Mol. Biol.*, in press